Oxazoline Functionalized Polystyrene as a Compatibilizer for Dispersion of Organoclay in Polyphenylene Ether Blends

Nivedita Sangaj,[1]* Amol Mohite,[1] G. Sadasivam,[1] Sushmita Franklin,[1] Hua Guo[2]**

[1]*GE Global Research, John F Welch Technology Centre, 122, EPIP Phase II, Whitefield Road, Bangalore-560066, INDIA*
[2]*SABIC Innovative Plastics, 1, Noryl Avenue, Selkirk, New York 12158*

Received 31 July 2009; accepted 7 January 2010
DOI 10.1002/app.32049
Published online 29 March 2010 in Wiley InterScience (www.interscience.wiley.com).

ABSTRACT: Addition of external additives as compatibilizers is known to improve exfoliation of nanoclay in various polymeric matrices. This study found that oxazoline functionalized polystyrene (OPS) is an effective compatibilizer to improve the dispersion of organoclay (Cloisite 20A) in polyphenylene ether (PPE)-based blends. The main objective of this study was to understand the mechanism of OPS as a compatibilizer for dispersion of nanoclay in PPE-based blends and evaluate whether the master-batch of organoclay in OPS can be used to disperse nanoclay in various PPE-based blends irrespective of the type of the other polymer component in the blend. Although the addition of OPS to polystyrene (PS) alone resulted in mere intercalation of organoclay, its addition to PPE-based blends was found to result in mixed clay dispersion of intercalated, exfoliated, and to some extent collapsed phases. Addition of OPS-organoclay combination in master-batch mode showed similar results as direct mode addition. At least 15% of OPS was required for effective dispersion of Cloisite 20A in PPE-high impact polystyrene blend. The possible role of solubility of OPS in the matrix and high melt shear of PPE-based matrix was investigated to understand the exclusive action of OPS in PPE-based blends. X-ray diffraction and transmission electron microscopy techniques were used to study the organoclay dispersion. Further master batches of organoclay in neat OPS and OPS containing PPE-based blends were evaluated in other PPE-based commercial blends. Of the various blends studied, blend containing phosphite additive showed better dispersion of organoclay. J Appl Polym Sci 117: 1718–1730, 2010

Key words: nanocomposite; compatibilizer; PPE blends; compatibility; organoclay

INTRODUCTION

Nanoclay-based composites can show true potential of reinforced nanometric sized clay particles when the individual clay particles are separated from each other and distributed randomly in all possible directions in a polymer matrix—a state known as "Exfoliated state."[1,2] Various factors such as polarity of nanoclay/organoclay and matrix, polymer-organoclay interaction, molecular weight (MW) of polymer, thermodynamic properties of the system, and processing conditions can influence the final dispersion of nanoclay in the matrix.[2–4] An approach of addition of external agents known as compatibilizers, swelling agent, or cointercalants has been used to improve the dispersion of nanoclay in various matrices.[5] These compatibilizers can be low MW compounds like epoxy, silicone fluid, or oligomeric additives such as polycaprolactone, functionalized polymers.[6–8] Inclusion of functionalized oligomeric polyolefins such as maleic anhydride grafted polypropylene (PP-g-MA) was found to improve the exfoliation of nanoclay in PP matrix.[9,10] The mechanism by which polymeric compatibilizers improve the dispersion of organoclay is believed to be similar to that of compatibilizer used to compatibilize two immiscible polymers in a blend system.

Compared with highly polar pristine Na-montmorillonite (Na-MMT) nanoclay, the treated nanoclay, i.e., organoclay, is apolar. However, the hydrophobicity of these clays is not sufficient to compatibilize and disperse them in majority of the polymers that are hydrophobic in nature. Polymeric or oligomeric compatibilizers contain polar functionalities such as maleic anhydride, hydroxyl, or amino groups that can interact with the nanoclay platelets, whereas the remaining nonpolar chain of the compatibilizer remains miscible with the polymer matrix.[11] This two-way interaction helps in overcoming the polarity

**Present address: Department of Bioengineering, University of California, San Diego, La Jolla, CA-92093, USA.*
***Present address: Indian Institute of Science, Bangalore - 560 012, INDIA.*
Correspondence to: A. Mohite (amol.mohite@ge.com).

mismatch between organoclay and polymer matrix and aids in the dispersion of organoclay in the system. The suitability of the polymeric compatibilizer depends on its interaction with preintercalated clay, miscibility in the matrix, ability to entangle with the matrix, etc. Because of polar interaction with the clay surface, compatibilizer helps in separating the nanoclay particles from the stacks thereby facilitating the diffusion of polymer molecules between the clay layers.[2]

Most of the commercially available organoclays are based on quaternary ammonium modifiers having tallow chain substitution. These organoclays have limited thermal stability (<220°C) depending upon the type of the organic treatment.[12] The lower thermal stability of ammonium organoclays limits their usage in engineering polymeric matrices that require higher processing temperature (usually above 240°C). Despite these limitations, better dispersion of organoclay in engineering polymer matrices can be obtained by judicious use of compatibilizers, e.g., use of telechelic ionomers helps in exfoliation of organoclay in PET matrix.[13]

Polyphenylene ether (PPE) is an engineering polymer with good dielectric properties, thermal, and hydrolytic stability.[14] PPE, also known as polyphenylene oxide, is often blended with styrenic polymers or polyamide to improve the processibility and mechanical properties. PPE blended with styrenic polymers like polystyrene (PS) or high impact polystyrene (HIPS) is very hydrophobic and generally processed at temperature above 270°C depending on the styrenic content. Higher processing temperature and hydrophobic nature of PPE blends can limit the use of commercially available organoclays.

Styrene-2-isopropenyl-2-oxazoline copolymer, hereafter referred as oxazoline functionalized polystyrene (OPS) has been reported as a compatibilizer for atactic, syndiotactic PS, and to some extent PPE matrices as well. Addition of OPS was found to result in reduction in intensity of the first-order peak in X-ray diffraction (XRD) and some improvement in the mechanical properties of PS.[15] Hasegawa et al. suggested that the strong hydrogen bonding between oxazoline group and oxygen atoms of silicate in nanoclay is the driving force in delaminating and dispersing the clay particles in the matrix. In syndiotactic PS, addition of OPS resulted in most of the clay being exfoliated with smaller amount of nanoclay showing collapsed phase.[16,17] The effects of temperature and annealing time on the clay dispersion and resultant mechanical properties of syndiotactic PS nanocomposites have also been studied in detail. The best clay dispersion was observed with dimethyl benzyl hydrogenated tallow ammonium-based modifier. In all the cases, however, there was a partial collapse of the clay. It was also observed that addition of master batch of nanoclay in OPS was found useful in exfoliating clay in syndiotactic PS matrix.[17]

Toyota's patent mentions that inclusion of 5% parts of clay in neat OPS resulted in good dispersion of clay with improvement in modulus and barrier to gases by 50% and 60%, respectively.[18] Furthermore, the same patent describes the use of OPS as a compatibilizer to improve dispersion of nanoclay in PPE. Analogous to PP-based nanocomposites using PP-g-MA as a compatibilizer and considering the complete miscibility of PS with PPE,[19] we hypothesize that OPS can act as a compatibilizer in PPE-based systems because of its reported compatibility with PS.

This study was done to investigate the efficacy of OPS as a compatibilizer in PPE-based blends. Furthermore, the optimum amount of OPS required to disperse organoclay in PPE-based matrix was determined. Although it is reported that the addition of OPS results in the intercalation of the organoclay in PS matrix and its compatibility with PS helps in increasing the dispersion of organoclay in PPE-PS matrix, its efficacy in other PPE matrices is not studied.

Master batches in neat OPS and in PPE-high impact polystyrene (HIPS)-OPS containing organoclay in intercalated and exfoliated forms, respectively, were used to disperse organoclay in other representative PPE-based blend systems such as PPE-polyamide and PPE-styrene block copolymer blends. The objective was to understand whether the master-batch approach can be used to disperse organoclay in various PPE-based compositions irrespective of the type of other polymer component of the blend. High efficacy of OPS as a compatibilizer observed preferentially in PPE-based matrix compared with PS was further investigated for the role of miscibility of OPS in the matrix by transmission electron microscopy (TEM) technique. To study the possible role of high melt shear of PPE-based matrix, comparison was done with high-melt viscosity polyetherimide (PEI)-based composition.

EXPERIMENTAL

Materials

PPE (grades PPE800, PPE803 of intrinsic viscosity (IV) 0.46, 0.41 dL/g, respectively) and PEI (grade Ultem*1010 with MW of 40 kDa) were obtained from SABIC Innovative Plastics, USA. HIPS (grade name SH-731) and Crystal clear PS (grade SC203EL) were obtained from Supreme Petrochemicals, India. Impact modifier styrene-ethylene-butylene-styrene copolymer (SEBS grade name Kraton G 1651) was obtained from Kraton Polymers, USA. OPS (EPOCROS RPS 1005) was obtained from Nippon Shokubai Co. Ltd., Japan. OPS (CAS # 30,174-74-4) contains 5% of vinyl oxazoline as a comonomer and has MW

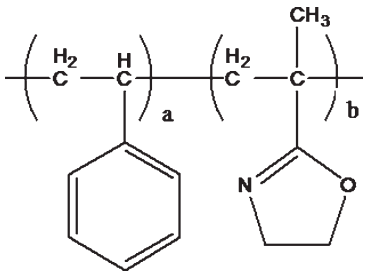

Scheme 1 Structure of OPS.

of 156,000 Da.[18] The structure of OPS is shown in Scheme 1. Polyamide 6 (Domamid 24) was obtained from Domo Chemicals, the Netherlands.

One representative grade from three classes of commercial grades was chosen for studying the effect of master-batch addition: (1) NORYL GTX* 934—a blend of PPE and polyamide, (2) NORYL* PX7511- PPE-HIPS blend, and (3) NORYL* WCD 891—a flexible blend of PPE, polyolefin, and styrenic elastomers. All the chosen grades were commercial materials and pigmented and obtained from SABIC Innovative Plastics, USA.

Nanoclays/organoclays used for this study are Na-montmorillonite-based Nanomer I.30T and Cloisite 20A. Nanomer I.30T is octadecyl amine modified organoclays organomodifier and procured from Nanocor Products, USA. Cloisite 20A is dimethyl dihydrogenated tallow quaternary ammonium salt modified organoclay obtained from Southern Clay Products, USA. Master batches of Cloisite 20A and Nanomer I.30T referred as MB1 and MB2, respectively, were prepared by adding 10% (w/w) of organoclay to OPS during melt extrusion at 210°C.

Processing

Twin-screw extruder configuration used for this study was 2-lobe–10 barrel screw of 25-mm diameter. Atmospheric and vacuum vents were located at sixth and nineth barrel, respectively. Weighed ingredients were mixed in a high-speed mixer and then melt-extruded. The maximum processing temperature for PPE-based formulations was 285°C, and the screw speed was 350 rpm. For PS-based formulations, the maximum processing temperature was 210°C, whereas PEI- and polyamide 6-based compositions were processed at 320°C and 260°C, respectively. PS- and polyamide 6-based compositions were extruded at a screw speed of 300 rpm, and PEI-based compositions were processed at 350 rpm.

The extrudate was chopped into pellets and subsequently dried at 85°C in an air-circulating oven. The dry pellets were injection molded using a LTM Demag 60-ton injection-molding machine into standard test specimens.

Characterization

Thermogravimetric analysis (TGA) of organoclays was done using Hi-Res TGA 2950 thermogravimetric analyzer (TA Instruments, India) under nitrogen atmosphere. Heating was ramped from room temperature to 800°C at a rate of 20°C/min.

Wide-angle X-ray spectroscopy (WAXD) or XRD was used to determine the d-spacing or the state of dispersion of the clay in the nanocomposite. XRD studies were done using a Panalytical X'Pert Pro X-Ray diffractometer (PANalytical India) in a reflection mode. The source was Cu K-α radiation of wavelength 1.54 Å. The scans were taken between 2θ values of 1.5–10° with a step size of 0.021 and time per step of 10.16s. Molded tensile specimens were used for XRD.

Validation studies were done by TEM on a Phillips CM-12 microscope. Samples for TEM observation were prepared by cutting, blocking, and facing of molded specimens on a Leica UCT ultramicrotome at room temperature. Multiphase systems were studied by staining the samples. Blocked samples were stained in Osmium tetroxide (OsO_4) solution at 70°C for 4 h. Few samples were also stained with Ruthenium tetroxide (RuO_4) vapors at 40°C for 90 s. Final microtomy of 100-nm sections was performed at room temperature on the Leica UCT.

Testing

Tensile test

The tensile tests were conducted in accordance with ISO527 using standard specimens. The test was conducted on Instron 5566 machine. The initial crosshead speed was 1 mm/min until a strain of 0.5% and then ramped to 50 mm/min until the failure of the specimens. Average of five specimens with standard deviation was reported.

Flexural modulus

Flexural modulus was measured as per ISO178 test method using Zwick/Roell Z010 universal testing machine. The strain rate was 2 mm/min. Average value of three specimens with standard deviation was reported in GPa.

Notched Izod impact (NII)

The NII test was conducted in accordance with ISO180 using standard specimens on Ceast-make machine. Average values from testing eight specimens were reported in kJ/m^2.

RESULTS AND DISCUSSION

The suitability of OPS as a compatibilizer has been reported for PS-based nanocomposites and to some

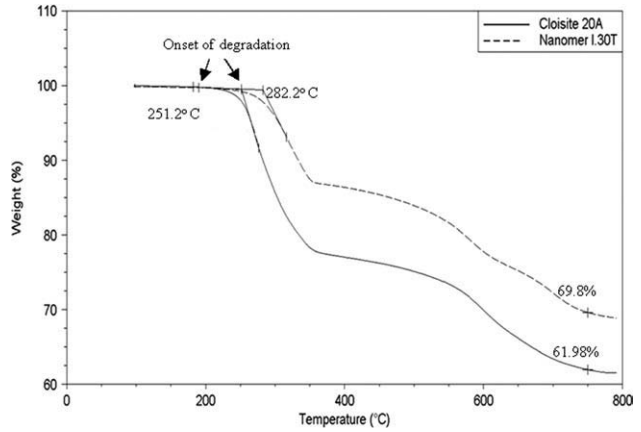

Figure 1 TGA scans of organoclays in N_2 showing onset of degradation (as measured by 1% weight loss) and residue at 750°C.

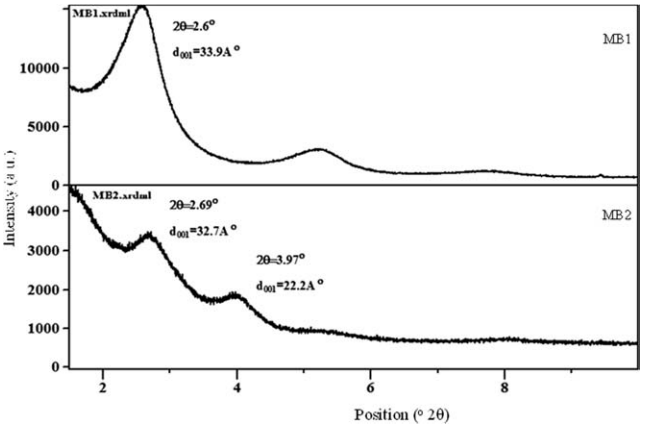

Figure 3 XRD patterns of master batches of organoclays in OPS—MB1: Cloisite 20A in OPS and MB2: Nanomer I.30T in OPS.

extent PPE-based nanocomposites as well. This study was done to understand the efficacy and mechanism of OPS as a compatibilizer in the dispersion of organoclay in PPE-based systems. In addition to this, the master-batch route of addition of organoclay has been investigated to achieve better dispersion of organoclay in various PPE-based blends irrespective of the composition of the blends.

Efficacy of OPS- direct and master-batch addition

The comparative TGA data of organoclays shown in Figure 1 clearly indicate that Nanomer I.30T is thermally more stable compared with Cloisite 20A. Onset of degradation for Cloisite 20A and Nanomer I.30T based on 1% weight loss on heating was found to be at 251.2 and 282.2°C, respectively. This trend agrees well with the lower thermal stability of quaternary ammonium salt compared to primary amine.[5,20] Weight loss at 750°C corresponds to inorganic content or complete degradation of organic modifier present in the organoclays—38.02 and 30.2% for Cloisite 20A and Nanomer I.30T, respectively, indicating higher amount of organic modifier in Cloisite 20A compared with Nanomer I.30T. Figure 2 shows XRD data of neat organoclays. The first-order d-spacings (d_{001}) of Cloisite 20A and Nanomer I.30T are 25.05 and 20.92 Å with the corresponding 2θ values of 3.5 and 4.2°, respectively.

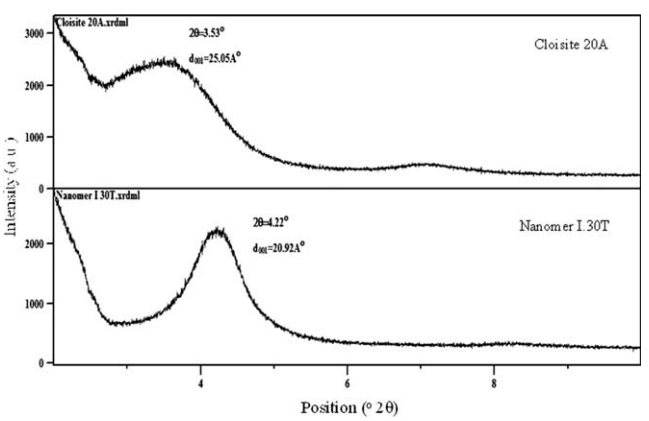

Figure 2 XRD patterns of neat organoclays.

On the basis of reported compatibility of OPS in PS, the miscibility of PS in PPE coupled with oxazoline functionality present on OPS that can interact with organoclay, addition of OPS is expected to aid in dispersion of organoclay in PPE-based blends. Evaluation of OPS as a compatibilizer was done initially in PPE (PPE803)-based formulations both by direct addition and master-batch addition to compare the effect of mode of mixing. In the direct addition method, OPS was added along with organoclay to PPE during the extrusion. In the master-batch approach, OPS was mixed with 10% organoclays and extruded at 210°C in the first pass. This master batch was then added to PPE matrix in the second pass process. Figure 3 shows the XRD patterns of Cloisite 20A master-batch (MB1) and Nanomer I.30T master batch (MB2).

As can be seen in Figure 3, both organoclays do not get exfoliated in neat OPS matrix under given conditions. In MB1, Cloisite 20A is in intercalated state with increased d-spacing from 25.05 to 33.9 Å. Moreover, the order in the organoclay is maintained over the long range as is evident from the second- and third-order peaks at 2θ values of 5.2 and 7.7°. MB2 shows less intense peaks compared with MB1. The d_{001} has increased from 20.92 to 32.7 Å ($2\theta \sim 2.69°$) whereas the second peak is at 2θ value corresponding to the additional clay phase having d-spacing of 21.9 Å.

In the second pass, these master-batches MB1 and MB2 were added to PPE-OPS blend to get the final organoclay loading of 3%. In both approaches, the

TABLE I
PPE-OPS-Based Nanocomposites Prepared by Master-Batch and Direct Addition Routes

	NOPS-1	NOPS-2	NOPS-3	NOPS-4
Components				
PPO803	64.7	64.7	64.7	64.7
OPS	32.3	32.3	5.3	5.3
Cloisite 20A	3			
Nanomer I.30T		3		
MB1			30	
MB2				30
Total	100	100	100	100
Properties				
E modulus (GPa)	3.15	3.07	3.16	3.09
Standard deviation	0.002	0.03	0.05	0.02
Tensile strength (MPa)	45.5	62	67.3	76.5
Standard deviation	7	5.6	3.7	3.4
Strain at break (%)	2.1	3.3	3.6	4.4
Standard deviation	0.4	0.3	0.2	0.4
Flexural modulus (GPa)	3.01	2.95	3.02	2.91
Standard deviation	0.09	0.02	0.006	0.02
NII strength (kJ/m^2)	1.98	2.30	2.04	2.08
Standard deviation	0.25	0.05	0.2	0.1

ratio PPE to OPS was maintained at 2 : 1. Table I shows the formulation details and their respective properties and Figure 4 shows the XRD patterns of these formulations.

Cloisite 20A-based nanocomposites (NOPS-1 and NOPS-3) showed slightly higher tensile and flexural moduli compared with the corresponding Nanomer I.30T-based formulations (NOPS-2 and NOPS-4). However, the standard deviation in tensile strength was higher, and based on average values, the trend seems to be quite opposite to that of modulus. The higher tensile strength observed with Nanomer I.30T-based formulations could be due to the possible reaction of oxazoline functionality with primary amine of the compatibilizer that can increase the interfacial strength between the dispersed fraction of organoclay and the matrix.[21] Both strain at break values and NII strength values of all the formulations indicate that nanocomposites are brittle in nature.

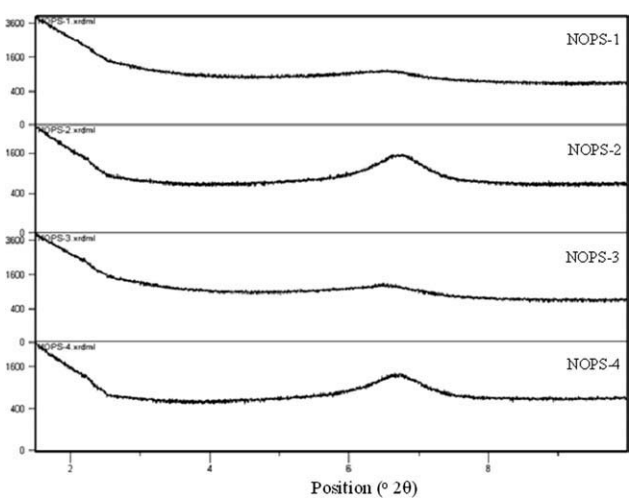

Figure 4 XRD patterns of PPE-based nanocomposites NOPS-1 to NOPS-4 prepared by direct addition and master-batch addition routes.

Formulations NOPS-1 to NOPS-4 showed different clay dispersions in XRD (Fig. 4) compared with those of MB1 and MB2. All the nanocomposites show peaks of varying intensity at ~2θ values of 6.5–7.5 corresponding to d_{001} of 13.2–13.6 Å indicating the presence of aggregated or collapsed phase. However, the peak associated with the collapsed phase is more intense for Nanomer I.30T-based formulations (NOPS-2 and -4) than the Cloisite 20A-based NOPS-1 and -3. Dispersion of organoclays in NOPS-1 to -4 is further validated by TEM as shown in Figure 5.

NOPS-2 and 4 showed the presence of bigger aggregated clay particles (darker regions), whereas comparatively NOPS-1 and -3 showed smaller clay stacks along with few clay particles uniformly distributed in the matrix. Lower d-spacing as observed in XRD and larger stacks of clays observed in TEM clearly show that Nanomer I.30 gets collapsed in PPE-based matrix. On the other hand, Cloisite 20A is a better organoclay than Nanomer I.30T in PPE-OPS formulations. Comparison of NOPS-1 and -3 with corresponding NOPS-2 and -4 indicate that the mode of addition of OPS as a compatibilizer makes little difference in the dispersion of organoclay and mechanical properties of nanocomposites. The differential dispersion of thermally less stable Cloisite 20A compared with Nanomer I.30T indicates that mere

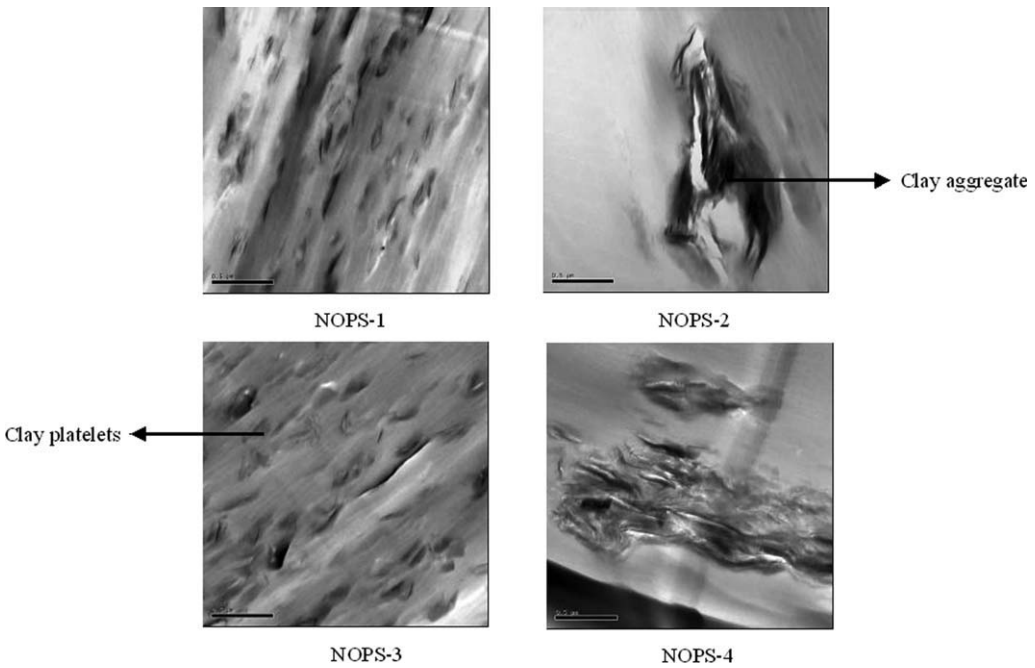

Figure 5 TEM images of nanocomposites NOPS-1 to -4 showing better dispersion of Cloisite 20A compared with Nanomer I.30T (scale bar is 0.5 μm).

higher thermal stability of organoclay does not necessarily help in effective dispersion in polymer matrix. Addition of external compatibilizer like OPS can result in better dispersion of even thermally less stable organoclay. On the basis of these findings, Cloisite 20A was chosen for further studies.

Optimization of OPS content

To evaluate the optimum amount of OPS required to disperse organoclay in PPE matrix, OPS was added as a partial replacement of HIPS in PPE (PPE800)-HIPS blend. Considering the poor ductility of the earlier formulations (NOPS-1 to -4), impact modifier Kraton G1651 was added at five parts loading. Although the above study was done at the clay loading of 3%, for optimization purpose, higher loading of organoclay (5%) was selected based on our earlier findings that mechanical properties of nanocomposites were improved with increase in clay loadings. Up to 5% clay loadings, the modulus-ductility balance was maintained, whereas above 5% clay

TABLE II
PPE-Based Nanocomposites Containing OPS as a Modifier at Various Loadings

	NOPS-5	NOPS-6	NOPS-7	NOPS-8	NOPS-9	NOPS-10
Components						
PPO800	60	60	60	60	60	60
HIPS	30	22.5	15	7.5		
OPS		7.5	15	22.5	30	
PS						30
Kraton G 1651	5	5	5	5	5	5
Cloisite 20A	5	5	5	5	5	5
Total	100	100	100	100	100	100
Properties						
E modulus (GPa)	2.93	2.82	2.9	2.97	3.12	3.21
Standard deviation	0.02	0.01	0.03	0.02	0.01	0.03
Tensile strength (MPa)	52.3	55.4	57.3	61.3	66.05	51.1
Standard deviation	0.8	1.2	1.2	1.9	1	7.2
Strain at break (%)	23	12.7	10.4	8.1	7	18.4
Standard deviation	1.9	1.1	0.9	0.7	0.3	1.1
Flexural modulus (GPa)	2.78	2.68	2.71	2.85	2.88	3.06
Standard deviation	0.004	0.03	0.03	0.01	0.01	0.02
NII strength (kJ/m^2)	22.3	5.8	4.6	4	2.6	7.3
Standard deviation	2	0.8	0.3	0.3	0.3	0.7

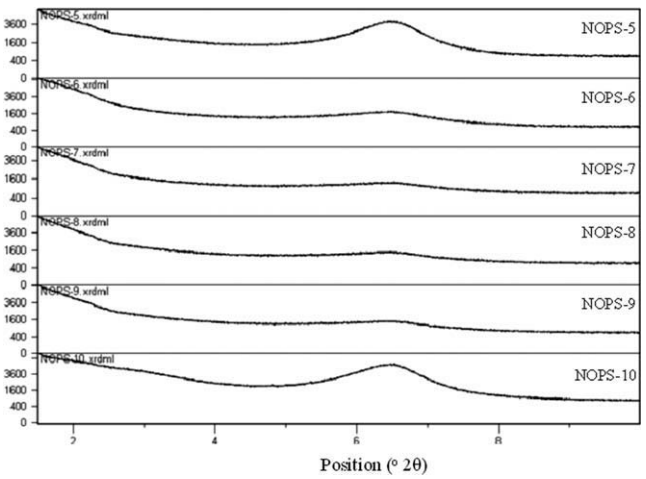

Figure 6 XRD patterns of nanocomposites NOPS-5 to -10 indicate that the aggregation of organoclay observed in NOPS-5 was significantly reduced by addition of OPS.

loading the reduction in elongation at break and impact strength was drastic.[22] Thus, 5% clay loading would be the maximum clay content for obtaining balanced mechanical properties. For optimization of OPS content, the replacement of total HIPS content with OPS was done at 0, 25, 50, 75, and 100%. In addition, one formulation with PS instead of HIPS was prepared for comparison. Table II shows formulations based on Cloisite 20A and OPS and their respective mechanical properties.

NOPS-5 without OPS showed the highest elongation at break values in the series followed by NOPS-10. The rest of the formulations containing similar organoclay loadings but various OPS loadings showed lower strain at break and notched izod impact strength. Tensile modulus and strength increased with increase in OPS loadings. This increment could be due to the effect of better-dispersed organoclay in the matrix. The NII strength was poor for all the formulations except for NOPS-5. The dispersion of Cloisite 20A in the formulations is determined by XRD, and Figure 6 shows the XRD data of these formulations.

In NOPS-5 and 10 compositions clay was in collapsed form as was evident from the intense and broad peak in the region of 2θ values of 5.5–8. With inclusion of 7.5% OPS (25% of HIPS content) as a compatibilizer in NOPS-6 the peak intensity reduced markedly indicating reduced aggregation of organoclays. As OPS loading increased further the peak intensity reduced further up to 15% loading and above this, clay dispersion did not seem to improve much. From the trend in XRD, it seems that OPS loading at 15% is suffice to achieve better dispersion of organoclay, and above this loading, the dispersion does not seem to improve further at least in XRD. In other words, considering the oxazoline content (5%) of OPS, at least 0.75% oxazoline content, is required to disperse organoclay effectively in PPE-HIPS blend.

Role of miscibility of OPS in PS and PPE-based nanocomposites

Because of the compositional similarity of OPS to PS matrix and the miscibility of PS with PPE, it is expected to function similar to PP-g-MA as a compatibilizer in PP matrix. To understand whether the exact mechanism of OPS as a compatibilizer is similar to that of PP-g-MA in PP-based matrices, OPS was used as a compatibilizer in PS-based nanocomposite. A total of 15% loading of OPS was chosen based on the better clay dispersion observed in XRD scan of NOPS-7 (Fig. 6), whereas the clay loading was of 3%. Formulation (NOPS-11) containing PS, OPS, and Cloisite 20A (in 82:15:3) was extruded at 210°C. As seen from the XRD scan of NOPS-11 in Figure 7, Cloisite 20A is in intercalated state with increased d-spacing from 25.0 to 33.2 Å, whereas the degree of ordering is maintained over the longer range as observed from second- and third-order peaks. This clearly indicates that in PS matrix, OPS is not effective compatibilizer to exfoliate clay.

The role of miscibility can be further investigated by TEM. RuO_4 was used to stain aromatic moieties, whereas for phase containing unsaturation such as HIPS, OsO_4 was used. Formulations NOPS-1 and NOPS-11 were stained with OsO_4 first and then with RuO_4 for TEM analysis. Figure 8 shows images of NOPS-1 and -11 stained with OsO_4 (images 1-a and 11-a) and successively with RuO_4 (images 1-b and 11-b). NOPS-11 images (NOPS-11-a and NOPS-11-b) seem to show the darker regions of clay particles, and there is no apparent density difference in the remaining phase. The darker regions of clay particles are owing to the stacked organoclay compared

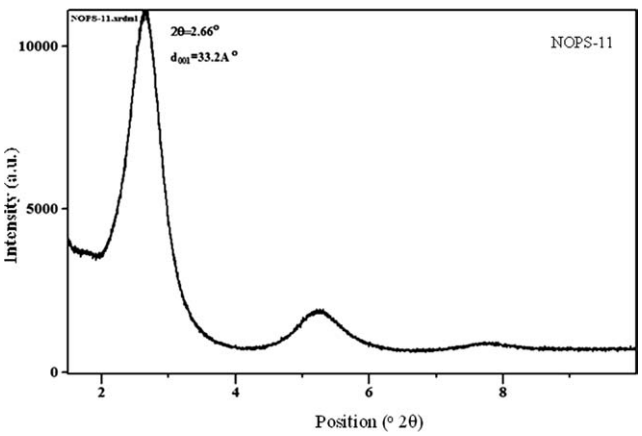

Figure 7 XRD pattern of OPS containing PS nanocomposite (NOPS-11) indicates intercalation of Cloisite 20A. Gallery spacing is maintained over the long range as seen by second and third-order peaks.

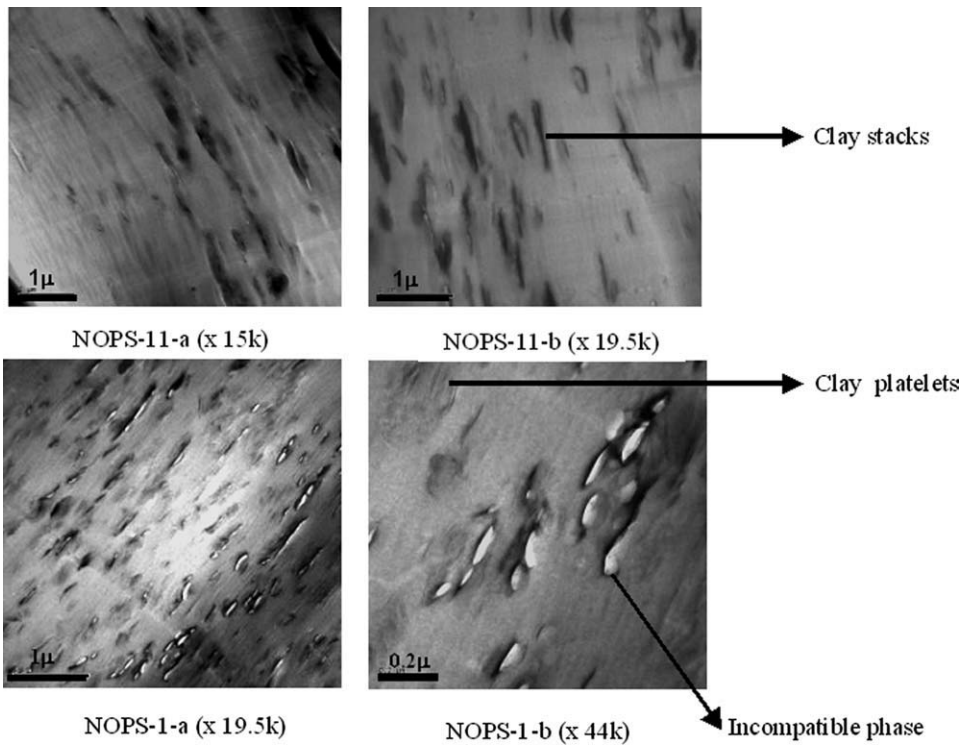

Figure 8 TEM images of PS nanocomposite (NOPS-11) and PPO nanocomposite (NOPS-1): NOPS-1-a and NOPS-11-a are OsO_4-stained images, whereas NOPS-1-b and NOPS-11-b are images of RuO_4-stained samples. NOPS-11 shows lighter regions of incompatible phase as against single phase NOPS-1.

with that observed for thinner clay particles in NOPS-1. On the basis of the thickness of the stacks and d-spacing observed for NOPS-11, the number of particles in the stacks ranges from 15 to 60. On the other hand, NOPS-1-a and NOPS-1-b show some additional lighter phase compared with the unstained images (Fig. 5). In NOPS-1-a, this lighter phase seems to be in the vicinity of clay particles. Although PS is completely miscible with PPE in all proportions, OPS shows some regions of immiscibility in PPE-based matrix. TEM images apparently show the inhomogeneity of OPS phase in PPE matrix and thus ruling out complete miscibility of OPS in PPE matrix. More experiments with controlled staining for various durations for TEM may help in discerning these nanocomposites. Presence of OPS in the vicinity of the organoclay in NOPS-1-a indicates interaction between OPS and organoclay. On the basis of these findings, it can be speculated that OPS helps in intercalation of organoclay because of polar interaction with the clay surface which then facilitates its final dispersion in PPE matrix as shown schematically in Figure 9.

Role of melt shear in dispersion of organoclay

In addition to the favorable interaction of organoclay with the matrix, the melt shear is known to play a significant role in the dispersion of organoclay.[23] Whether the exclusive action of OPS compatibilizer in PPE-based system is due to high-melt viscosity of the PPE-based matrix compared with PS that helps in peeling of the individual clay particles from the tactoids can be assessed by adding OPS master batch to another high shear matrix. PEI was chosen as a

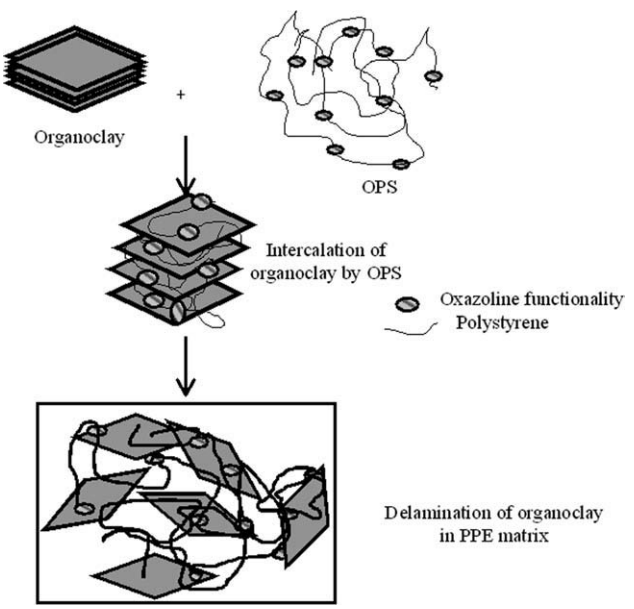

Figure 9 Schematic showing the plausible action of OPS as a compatibilizer in PPE matrix.

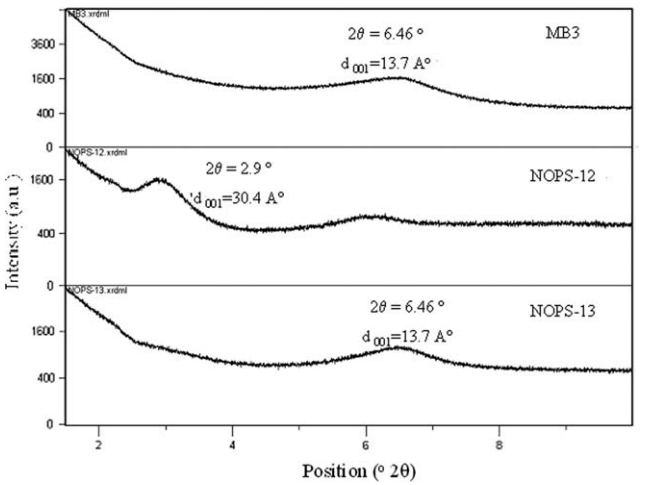

Figure 10 XRD patterns of master batch (MB3) of Cloisite 20A in PPO-HIPS-OPS and PEI nanocomposites (NOPS-12 and -13) prepared by using master-batches MB1 and MB3, respectively.

matrix to understand the role of melt shear on the action of compatibilizer. PEI (Ultem1010) is an engineering polymer having high melt viscosity, e.g., melt viscosity of Ultem1010 at 320°C and a shear rate of 1000 s^{-1} is 722 Pa-S while that of NOPS-5 (PPE/HIPS/SEBS blend) without organoclay at 285°C and 1000 s^{-1} is 430 Pa-S. Similar to NOPS-11 only clay dispersion was studied for this matrix. Two master batches—based on OPS (i.e., MB1) and another PPE-based master batch (MB3) containing PPE/HIPS/OPS/Cloisite 20A in 65 : 15 : 15 : 10 ratio—were used. Loading of 15 parts of OPS was chosen based on the optimization study of OPS. Individual master batch was added to PEI in 70 : 30 ratio and melt extruded at 320°C. MB1-based formulation (NOPS-12) showed severe melt degradation during extrusion, whereas MB3 containing formulation (NOPS-13) showed comparatively less thermal degradation. XRD scans of both these formulations are represented in Figure 10, and comparative d-spacing of various nanocomposites are shown in Table III.

NOPS-12 showed first-order peak at 2θ value of 2.9° that corresponds to the d-spacing of 30.4 Å—less than the d-spacing of MB1 (33.9 Å). On the other hand, NOPS-13 retained the same similar d-spacing as that of added MB3. In case of NOPS-12, it is difficult to speculate on the role of melt shear of the PEI or lack of it due to the observed reduction in the melt viscosity during extrusion. In NOPS-13, this reduction in the melt viscosity was less compared with NOPS-12, and hence, clay dispersion could be either or both due to high-melt viscosity of the PEI or MB3 as such. To verify the extent of dispersion of Cloisite 20A in PEI matrix, TEM images were taken after staining the samples. Figure 11 shows TEM images of NOPS-13 unstained and stained with OsO_4 (NOPS-13-a) followed by RuO_4 (NOPS-13-b).

In NOPS-13-a image, the clay particles are seen aggregated in immiscible region and considering salami structure of HIPS in this region, this immiscible phase seems to be of PPE-HIPS master-batch phase. In RuO_4-stained NOPS-13-b image, clearly segregated, immiscible, and darker regions of PPE-HIPS phase appear in the PEI matrix. Thus, the retained state of dispersion of Cloisite 20A in NOPS-13 as seen in XRD does not imply that the organoclay is dispersed to the same extent as in master-batch MB3. The addition of MB1 and MB3 to PEI does not result into the same level of clay dispersion as observed in PPE-HIPS matrices. Rather the dispersed clay remains confined in the immiscible phase of PPE-HIPS in PEI matrix.

The role of melt shear in the exfoliation of clay could not be ascertained because of thermal degradation observed in the PEI matrix. On the basis of the reported compatibility of PS in OPS, preferential action of OPS in PPE-HIPS matrix over PS and thermodynamic instability of PPE-OPS MB in the PEI, it can be said that the action of OPS could be due to combined action of partial solubility in the matrix, high melt shear, and favorable interaction of oxazoline functionality with organic modifier of the organoclay. The increased separation between the clay platelets due to polar interaction between oxazoline and organoclay and high melt shear of PPE matrix can aid in molecular diffusion of PPE between the

TABLE III
Comparative Values of 2q and d-Spacing of Organoclays, Their Master Batches and PPE and Ultem 1010-Based Blends

Description	Composition	2θ (°)	d (Å)
Cloisite 20A	Cloisite 20A	3.53	25.05
Nanomer I.30T	Nanomer I.30T	4.22	20.92
MB1	OPS/Cloisite 20A	2.6	33.9
MB2	OPS/Nanomer I.30T	2.69/3.97	32.7/22.2
MB3	PPE/HIPS/OPS/Cloisite 20A	6.46	13.7
NOPS-11	PS/OPS/ Cloisite 20A	2.66	33.2
NOPS-12	Ultem1010/MB1	2.9	30.4
NOPS-13	Ultem1010/ MB3	6.46	13.7

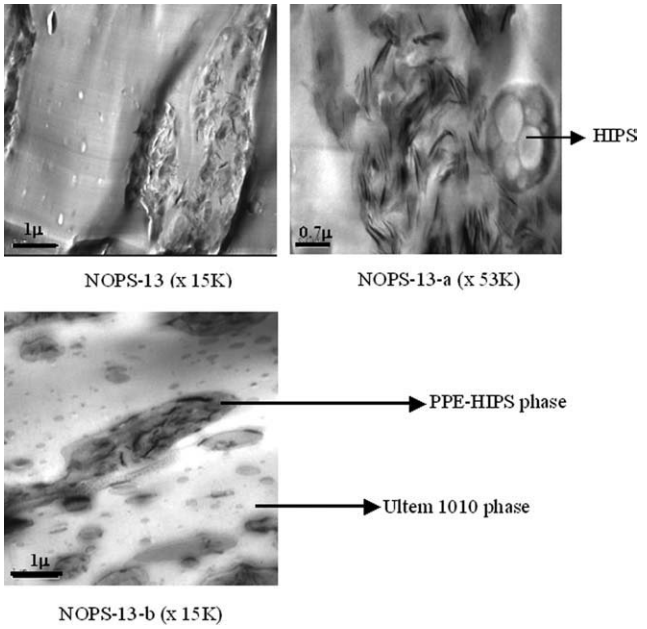

Figure 11 TEM images of PEI nanocomposites prepared by using master-batch MB3: NOPS-13 is unstained image, NOPS-13-a is OsO_4 stained image showing the presence of HIPS in the vicinity of organoclay, whereas NOPS-13-b is RuO_4-stained image indicating most of the clay confined in PPE-HIPS phase.

clay platelets and peeling off the clay platelets from the stacks.[24]

Master batch of organoclay in other PPE-based blends

Master batches of Cloisite 20A in OPS (MB1) and PPE-HIPS-OPS (MB3) were further used to disperse organoclay in commercial PPE-based formulations. The objective was to evaluate whether the master-batch approach can be used to disperse organoclay in various PPE-based blends—irrespective of the compositions. Three commercial Noryl grades chosen for this study were NORYL GTX* 934, NORYL* PX7511, and NORYL* WCD 891. The master-batch was mixed in 70 : 30 (commercial grade/master batch) and extruded. The effective loading of Cloisite 20A in the final blend was 3%. The molded specimens were characterized by XRD and TEM for determining the clay dispersion. The compositional details of the blends are shown in Table IV.

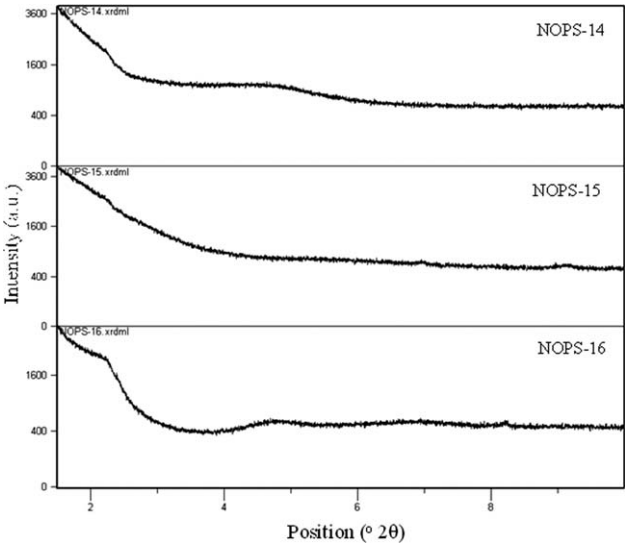

Figure 12 XRD scans of nanocomposites based on PPE-based grades prepared by addition of master-batch MB1: NOPS-15 shows better dispersion of organoclay, whereas NOPS-14 and NOPS-16 show mixed states of dispersion.

XRD scans of these formulations are as shown in Figures 12 and 13. Compared to the intercalated structure of clay in MB1, the state of clay dispersion changes when added to commercial grades. As seen in Figure 12, NOPS-14 showed a broad peak between 2θ values of 3.6–5.7°, which corresponds to organoclay with reduced d-spacing. NOPS-16 showed multiple peaks at 2.2, 4.7, and 6.9° values. On the other hand, NOPS-15 did not show any peak and seems to be in exfoliated state of organoclays. GTX934- and WCD891-based nanocomposites showed mixed morphology of collapsed and intercalated clays. However, the extent to which d-spacing was reduced in these formulations seems to be much less than that in NOPS-5 and -6 formulations.

As shown in Figure 13, formulation NOPS-18 showed peak at 2θ value of 6.5 Å corresponding to a collapsed organoclay phase. PPE-polyamide blend-based NOPS-17 showed slightly better dispersion without any significant peak. In NOPS-19,

TABLE IV
Compositions of Nanocomposites of PPE-Based Grades Prepared Using Organoclay Master Batch in OPs (MB1) and in PPO-HIPS-OPS (MB3)

Components	NOPS-14	NOPS-15	NOPS-16	NOPS-17	NOPS-18	NOPS-19
GTX 934	70			70		
PX7511		70			70	
WCD891			70			70
MB1	30	30	30			
MB3				30	30	30
Total	100	100	100	100	100	100

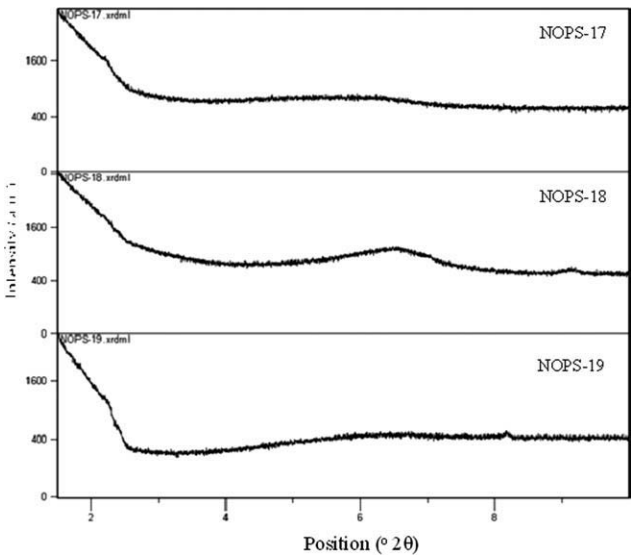

Figure 13 XRD scans of nanocomposites based on PPE-based grades prepared by addition of master-batch MB3 showing mixed states of dispersion of Cloisite 20A.

organoclay seems to be nearing to exfoliated state. To verify the dispersion of organoclay in these blends, multiple TEM images were taken. Figure 14 shows representative TEM images of formulations NOPS-14 to -16. NOPS-15 has shown fine clay particles in TEM images. The dark area (spots) in the image is due to pigment present in PX7411. NOPS-16 based on WCD891 and GTX934 based NOPS-14 show largely bigger clay stacks with some thinner clay particles. On the basis of the TEM observation, the clay dispersion seems to be in the following order: NOPS- 15 > NOPS-14 > NOPS-16.

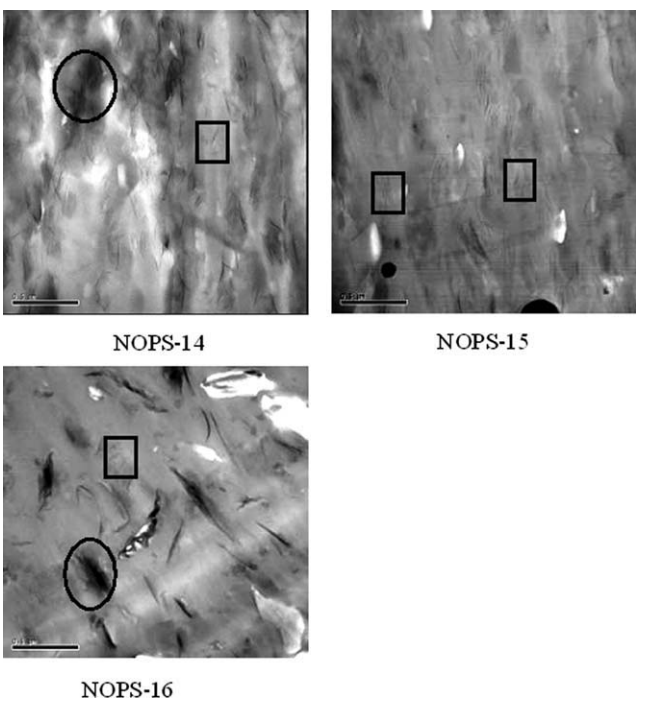

Figure 14 TEM images of nanocomposites NOPS-14 to -16 showing fine dispersion of organoclay (represented in rectangles) in NOPS-15 compared with bigger stacks (encircled) seen in NOPS-14 and -16 (scale bar is 0.5 m).

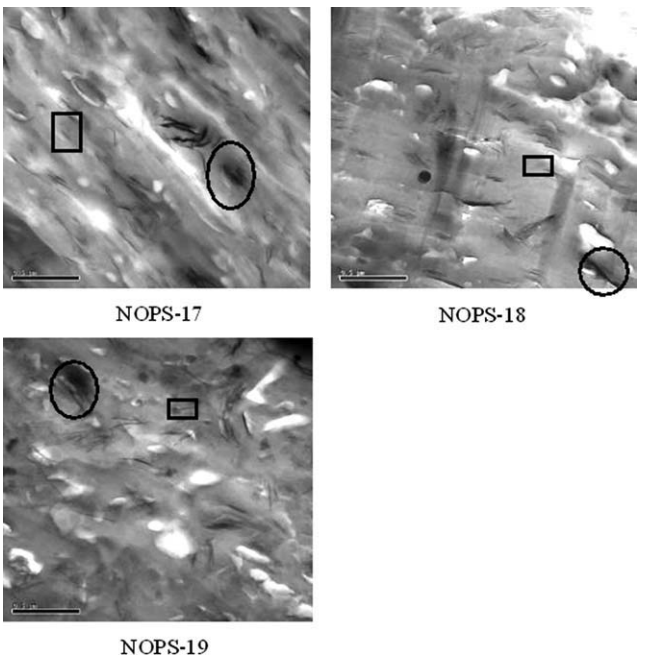

Figure 15 TEM images of nanocomposites NOPS-17 to -19 showing mixed states of dispersion of organoclay (fine dispersion as represented in rectangles and bigger stacks as encircled; scale bar is 0.5 m).

All the compositions based on MB3 showed (Fig. 15) mixed states of dispersion of organoclay, and none of them matched the dispersion shown by NOPS-15. NOPS-19 showed comparatively bigger tactoids compared with NOPS-17 and -18. The latter two showed thinner stacks and some individual clay platelets as well. The exfoliation observed in NOPS-15 was the best exfoliation that we have observed in PPE-based matrix so far. Typically, polyamide 6 matrix has been known to show ease and high level of exfoliation of organoclay.[25] To understand the level of clay dispersion in NOPS-15, XRD of NOPS-15 was compared with that of polyamide 6-based nanocomposite containing 3 parts of Nanomer I.30T as shown in the Figure 16. NOPS-15 shows similar XRD profile as that of polyamide 6-based nanocomposite.

Synergistic action of phosphite stabilizer

The surprisingly better exfoliation observed in NOPS-15 could be attributed to the presence of phosphite stabilizer—triisodecyl phosphite (TDP) in PX7411. Phosphorus-based compounds, such as phosphate, phosphite, etc., are known to improve the exfoliation of organoclay in PPE-based formulation.[26] Exceptionally good exfoliation in NOPS-15

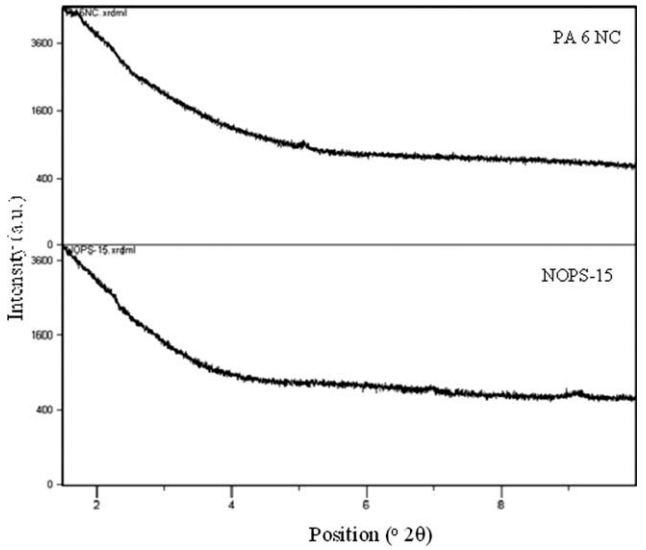

Figure 16 Comparative XRD patterns of NOPS-15 and polyamide 6-based nanocomposite indicating similar extent of organoclay dispersion.

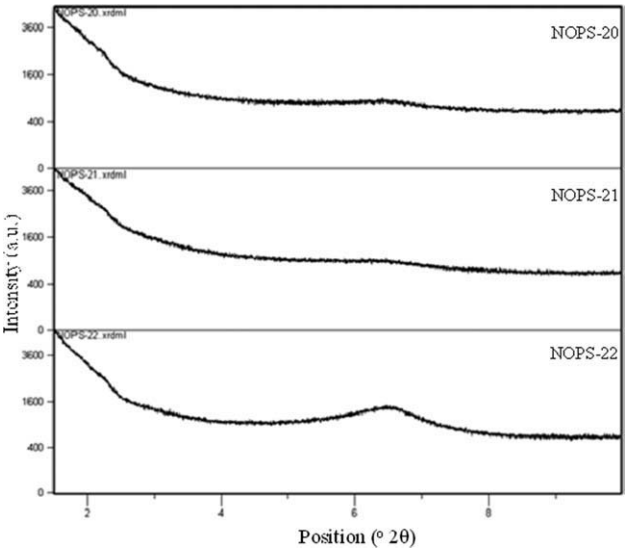

Figure 17 XRD pattern of NOPS-20 to -22 containing combination of OPS and TDP: NOPS- 20 and -21 show synergistic action of TDP and OPS on the dispersion of Cloisite 20A.

could be due to synergistic action of OPS and TDP in the formulation. Compared with NOPS-15, corresponding NOPS-18 based on MB3 showed a collapsed organoclay phase. This shows that organoclay that is intercalated in MB1 gets exfoliated in the presence of TDP in NOPS-15, but when MB3 is added to PX7411, organoclay is already partially collapsed or thermally degraded, and hence, TDP does not work effectively to the same extent as in NOPS-15.

The synergistic action of OPS and TDP was verified by adding OPS and TDP together to PPE-HIPS blend and comparing the organoclay dispersion with addition of TDP with MB1 and MB3. In all the formulations, the effective clay loading was 3%, whereas the total amount of PPE content was maintained same. Table V shows the blend compositions, and Figure 17 shows corresponding XRD data of these blends.

NOPS-20 and -21 showed better exfoliation compared with NOPS-22 based on MB3. The *in situ* addition of TDP-OPS combination works similar to TDP-MB1 combination. TDP is believed to have polar interaction with organic modifier of organoclays and thus aids in dispersion of organoclays in the PPE matrix.[26] The combination of these two additives results in the exfoliation of organoclay in PPE-based matrix. Addition of TDP seems to result in better delamination of organoclay in NOPS-21 in which the clay is in intercalated form in the added master batch (MB1). Conversely, in NOPS-22, the fraction of the clay in the master batch is already in the collapsed form, and hence, TDP does not seem to work effectively. The effect of improved dispersion of organoclay in various PPE-blends on their mechanical, thermal, and electrical properties is under further investigation.

TABLE V
PPE-HIPS-Based Nanocomposites Containing a Combination of OPS and TDP as a Modifier

Components	NOPS-20	NOPS-21	NOPS-22
PPO800	64.4	64.7	46.7
HIPS	16.1	4.8	23.3
OPS	16.1		
TDP	0.5	0.5	0.5
Cloisite 20A	3		
MB1		30	
MB3			30

CONCLUSIONS

OPS was found to be an effective compatibilizer to disperse organoclay in PPE-based matrix. Within the scope of this study, the following conclusions can be drawn: the optimum amount of OPS required for improved dispersion of organoclay in PPE-HIPS blend with was 15%. Mode of addition of OPS—either direct or in master-batch form—showed little difference on the dispersion of organoclay. Cloisite 20A showed mere intercalation when added directly to OPS. However, the same master batch when added to PPE-HIPS formulation showed exfoliation with some amount of collapsed clay.

Stained TEM images showed some indication of inhomogeneity of OPS in PPE-based matrix, although OPS showed complete homogeneity in PS matrix. This observation seriously limited the clarity on the effect of miscibility of OPS for its action as a

compatibilizer in PPE-based matrix. The role of high-melt shear viscosity of PPE-based formulations could not be ascertained because of thermal degradation of PEI-based nanocomposites on addition of OPS-based master batches. However, there is a possibility that action of OPS in PPE blends could be combination of these factors rather than a sole individual factor.

OPS showed synergistic action in combination with phosphite stabilizer TDP. The exfoliation observed in commercial PPE-HIPS-based blend containing TDP was the best in the series and matched with that of polyamide 6-based nanocomposites in XRD.

The authors thank Sho Sato (SABIC Innovative Plastics, Moka, Japan), John Yates (SABIC Innovative Plastics, Selkirk, USA), Satishkumar Mahanth, and Pallavi MB (GE Global Research, Bangalore, India) for their help and suggestions for this study.

References

1. Powell, C. E.; Beall, G. W. Curr Op Solid State Mater Sci 2006, 10, 73.
2. Pavlidou, S.; Papaspyrides, C. D. Prog Polym Sci 2008, 8, 1119.
3. Esfandiari, A.; Nazokdast, H.; Rashidi, A.; Yazdanshenas, M. J Appl Sci 2008, 8, 545.
4. Ray, S. S.; Okamoto, M. Prog Polym Sci 2003, 28, 1539.
5. Utracki, L. A. Clay-Containing Polymer Nanocomposites; Rapra Technology Ltd., UK, 2004; Vol. 1.
6. Bilotti E., H. R.; Fischer, H. R.; Peijs T. J Appl Polym Sci 2008, 107, 1116.
7. Ishida, H.; Campbell, S.; Blackwell, J. Chem Mater 2000, 12, 1260.
8. Hasegawa, N.; Kawasumi, M.; Kato, M.; Usuki, A.; Okada, A. J Appl Polym Sci 1998, 67, 87.
9. Pascual, J.; Fages, E.; Fenollar, O.; Garci'a, D.; Balart, R. Polym Bull 2009, 62, 367.
10. Kawasumi, M.; Hasegawa, N.; Kato, M.; Okada, A. Macromolecules 1997, 30, 6333.
11. Chung, T.; Manias, E.; Wang, Z. U.S. Pat. 7,241,829 B2 (2007).
12. Utracki, L. A.; Kamal, M. R. Arabian J Sci Engg 2002, 27, 43.
13. Barber, G. D.; Calhoun, B. H.; Moore, R. B. Polymer 2005, 46, 6706.
14. Brydson J, A. Plastics Materials, 7th ed.; Butterworth-Heinnemann: Oxford 1999.
15. Hasegawa, N.; Okamoto, H.; Kawasumi, M.; Usuki, A. J Appl Polym Sci 1999, 74, 3359.
16. Tanoue, S.; Hasook, A.; Itoh, T.; Yanou, M.; Iemoto, Y.; Unryu, T. J Appl Polym Sci 2006, 101, 1165.
17. Park, C. I.; Choi, W. M.; Kim, M. H.; Park, O. O. J Polym Sci Part B: Polym Phys 2004, 42, 1685.
18. Hasegawa, N.; Okamoto, H.; Kawasumi, M.; Usuki, A.; Okada, A. U.S. Pat. 6,117,932 (2000).
19. Yang, J.; An, L.; Xu, T. Polymer 2001, 42, 7887.
20. Cui, L.; Khramov, D. M.; Bielawski, C. W.; Hunter, D. L.; Yoon, P. J.; Paul, D. R. Polymer 2008, 49, 3751.
21. Frump, J. A. Chem Rev 1971, 71, 483.
22. Sangaj, N. S.; Sadasivam, G.; Mohite, A. A.; Franklin, S. Comparison of Nanoclays With Microfillers in Noryl* Classico'—internal technical report; GE GRC technical Report, Bangalore, India, 2008.
23. Fornes, T. P.; Yoon, H.; Keskkula, H.; Paul, D. R. Polymer 2001, 42, 09929.
24. Dennis, H. R.; Hunter, D. L.; Chang, D.; Kim, S.; White, J. L.; Cho, J. W. Polymer 2001, 42, 9513.
25. Paul, D. R.; Robenson, L. R. Polymer 2008, 49, 3187.
26. Kato, M.; Usuki, A.; Shirai, J.; Hiroyuki, W.; Osuka, K.; Sato, S.; Kitamura, T. U.S. Pat. 0,123,575A (2002).